Thin waveplate lenses - new generation in optics

Nelson V. Tabiryan*[a], Svetlana V. Serak[a], David E. Roberts[a], Diane M. Steeves[b], Brian R. Kimball[b]
[a]Beam Engineering for Advanced Measurements Co (BEAM Co.)., 1300 Lee Rd, Orlando, Florida 32810, USA; [b]US Army Natick Soldier Research, Development & Engineering Center, 15 General Greene Avenue, Natick, Massachusetts 01760, USA

ABSTRACT

We present new lenses – waveplate lenses created in liquid crystal materials. Waveplate lenses allowed focusing and defocusing laser beam depending on the sign of the circularity of laser beam polarization. Using an electrically-switchable liquid-crystal half-wave retarder we realized switching between focused and defocused beams by the waveplate lens. A combination of two such lenses allowed the collimation of a laser beam as well as the change of focal length of optical system. Lenses of varied size and focal length are presented.

Keywords: Lasers, diffractive gratings; lenses, liquid crystals; photochemistry

1. INTRODUCTION

Lenses are commonly made by shaping an optical material such as glass. The weight of such lenses increases strongly with diameter making them very expensive and prohibitively heavy for applications requiring large area. Also the quality of a lens typically decreases with increasing size. Diffractive lenses such as Fresnel lenses are relatively thin, however, the structural discontinuity adds to aberrations [1, 2]. Uses of holographic lenses are limited by the compromise of efficiency and dispersion [3]. Liquid crystal lenses have been developed intensively due to their capability to provide electrically-controllable focal length [4-12]. But those lenses had aberrations and need improvements of alignment quality during the switching process.

Thus, there is a need for switchable and non-switchable lenses that could be obtained in the form of thin film structurally continuous coatings on a variety of substrates.

We developed continuous thin film, ~1 μm thick, waveplate lenses, which can switch between concave and convex positions by control of light polarization sign. Lenses of various sizes, various focal lengths, from micrometers to meters, various parabolic structures, cylindrical, spherical of axicon configurations, for a wide wavelength range were created. Combinations of waveplate lenses with liquid crystal (LC) retarders allowed electrical switching between collimated and focused/defocused beams as well as control of focal length.

2. WAVEPLATE LENS CONCEPTION

Thin film cycloidal waveplate gratings were recorded by cycloidal distribution of beam polarization in one direction in liquid crystal materials [13-21]. Here we report two dimensional structures having parabolic distribution of orientation of director of liquid crystal (LC) molecules. Patterns of optical axis orientation demonstrating waveplate lenses performing the same optical function as a refractive lens with spherical or free-form surfaces are shown in Figure 1. The waveplate lenses (WLs) are fabricated using photoalignment of a liquid crystal (LC) or liquid crystal polymer (LCP). The polarization pattern of radiation used for photoalignment is obtained by propagating the light through an optical system comprising a shape-variant nonlinear spatial light polarization modulator [Figs. 1(b), 1(c)]. Recording cycloidal orienting conditions on a substrate coated with a photoaligning material film (PAAD) is shown in Figs. 1(d), 1(e).

*nelson@beamco.com; phone +1 (407) 734-5222; fax +1 (407) 969-0477; www.beamco.com

Liquid Crystals XIX, edited by Iam Choon Khoo, Proc. of SPIE Vol. 9565, 956512
 · doi: 10.1117/12.2190295

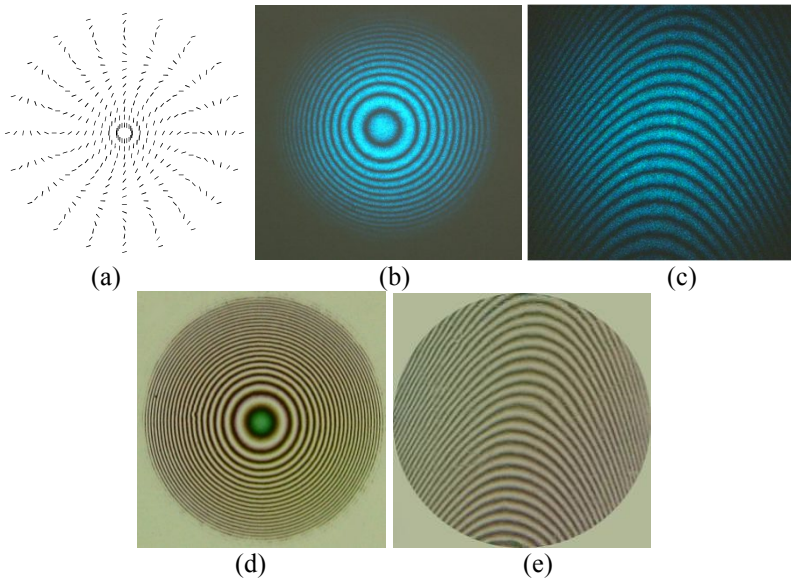

Figure 1. (a) Example of axially symmetric spatial distribution of optical axis orientation in a birefringent film, with orientation angle proportional to the square of the radial coordinate. (b, c) Laser beam patterns received at the output of the optical recording system. (d, e) Waveplate lenses equivalent to a refractor with spherical (d) and free-form (e) surfaces in nematic LC between polarizers.

To create waveplate lenses in liquid crystals materials, the thickness of LC layer L and its birefringence Δn must be such that the half-wave phase retardation condition $L\Delta n=\lambda/2$ is met, where λ is the operating wavelength.

3. EXPERIMENT and RESULTS

3.1. Waveplate lens fabrication in LC cell and LC polymer layer

The polarization modulation patterns were recorded on photoalignment material PAAD-72 (BEAM Co.). The PAAD layer is created on a glass substrate by spin-coating of 1% solution of PAAD-72 in DMF at a rotation speed 3000 rpm during 30 s. Then, the PAAD layer was exposed to the laser beam at wavelength corresponding to the absorption band of the PAAD material. The peak absorption of PAAD-72 occurs at a wavelength of 424 nm. An Argon ion laser operated at the wavelength of 488 nm was used for exposure. The exposure time was 10 min and beam intensity was 15 mW/cm^2. He-Ne laser beam at wavelength 633 nm was used for probing.

Photoaligned substrates were used for making liquid crystal cells. Empty LC cell was exposed to Argon ion laser beam to create polarization patterns in photoaligned material. Thickness of the cells corresponded to half-wave retardation condition for wavelength of 633 nm. Low birefringence BEAM Co. liquid crystal material R-237 (Δn=0.057) was filled in the gap between substrates. Orientation distribution of LC molecules in the cell corresponded to waveplate lens. Alternatively, the PAAD coated substrates were coated with a layer of liquid crystal monomer solution RLCS-7 (BEAM Co.). The layer of RLCS-7 was spin-coated on the PAAD-72 layer at a rotational speed of 3000 rpm for 1 min and then was cured with unpolarized UV light at 365 nm wavelength and intensity 90 mW/cm^2 with an exposure time of 5 min. The thickness of the polymer layer allowed creation of a half-wave phase retardation condition at 633 nm wavelength.

3.2. Optics of single waveplate lens

Figure 2 demonstrate structure of WL lens taken with 10X Olympus microscopic objective. Phase profile across the lens of 7-mm diameter in accordance to distance between rings, which was calculated from photomicrographs of the lens between crossed polarizers, is shown in Fig. 2(b). Number of rings corresponded to optical phase shift equal to 45π. Fitting of data with parabolic function demonstrates high symmetry and good agreement between the calculated optical phase and the parabolic phase model.

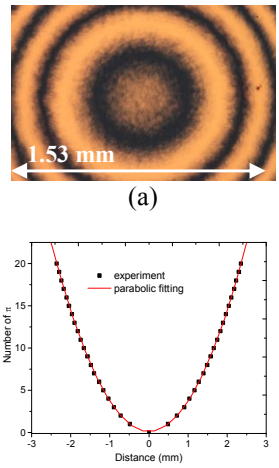

Figure 2. (a) Photo of waveplate lens taken with 10X Olympus microscope objective between crossed polarizers. (b) Experimentally measured dependence of phase shift on distance from the center of the waveplate lens and its parabolic fit.

Lenses of different focal length were recorded by simply changing the size of the polarization modulation pattern projected onto the photoalignment layer. Photos of waveplate lenses of different focal length and dependencies of focal length on lens diameter and spacing period are presented in Figure 3. Relationship between paraxial focal length F, grating period Λ on the edge, wavelength λ and lens diameter D can be calculated taking into account diffraction condition for grating period on the edge of the lens: $F=\Lambda D/2\lambda$. We also recorded lenses with smaller spacing period Λ=3.6 μm with focal length F=5.7 mm.

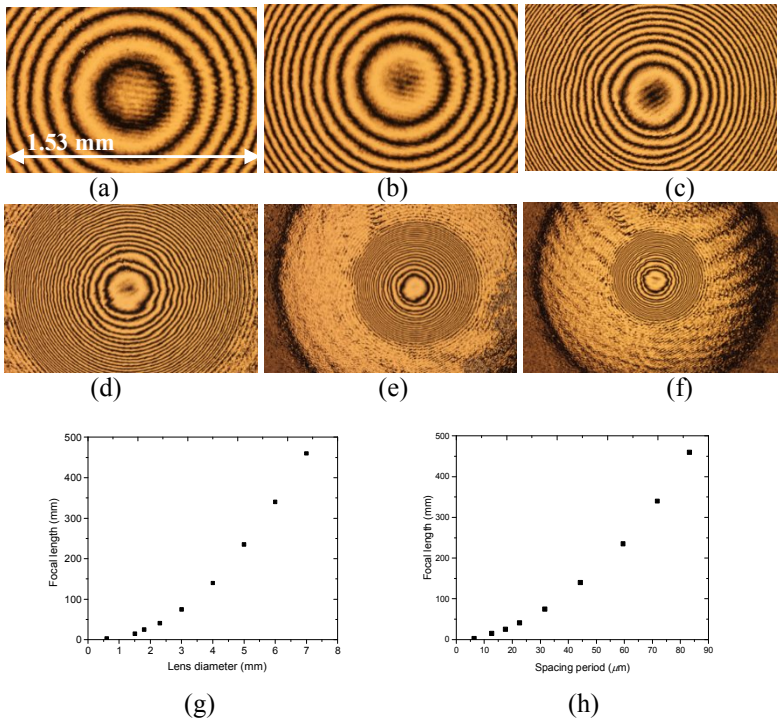

Figure 3. (a-f) Photos of waveplate lenses taken with 10X Olympus microscope objective between crossed polarizers: (a) lens diameter D = 4.7 mm, F = 230 mm; (b) D = 4 mm, F=140 mm; (c) D=3 mm, F=61 mm; (d) D=2.3 mm, F=32 mm; (e) D = 1.7 mm, F = 15 mm; (f) D=1 mm, F=5 mm. (g, h) Dependence of focal length on (g) lens diameter and (h) spacing period on the edge.

Expanded and collimated probe He-Ne laser beam passed through waveplate lens and was focused or defocused depending on circularity of beam polarization. The polarization of the light was switched from right-hand circular polarization (RHCP) to left-hand circular polarization (LHCP) by rotating the quarter-wave plate (QWP). The photo (b) in Figure 4 corresponds to linear polarized (LP) or unpolarized incident beam, the photo (c) corresponds to RHCP incident beam, and the photo (d) corresponds to LHCP beam. Two images corresponding to lenses with positive and negative focal lengths were observed simultaneously for linear polarized laser beam. When laser beam was RHCP, waveplate lens had a positive focal length, as if it was a convex (CX) refractive lens, and therefore converged the collimated input beam. When laser beam was LHCP, the waveplate lens was switched to having a negative focal length, as if it were a concave (CV) refractive lens, thus diverging the collimated input beam. Focal length of lens was switched between F_{CX}=190 mm and F_{CV}=-190 mm by switching the circular polarization of the probe beam. The sign of the focal length of the waveplate lens was changed from positive to negative for the same RHCP laser beam, when the lens was turned from face side to back side, Figs. 4(e), 4(f).

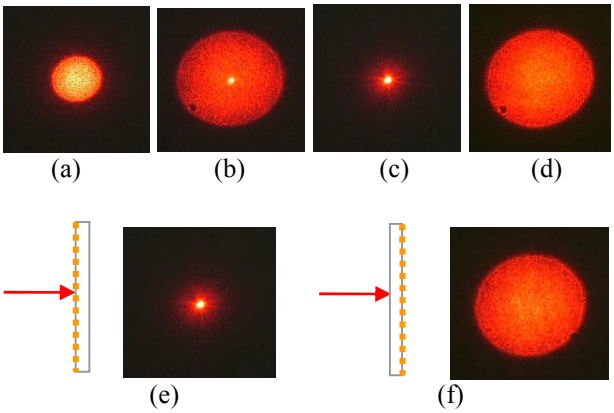

Figure 4. (a) Photo of laser beam on a screen. (b-d) Photos of beam image in the focus, when WL was set: (b) LP; (c) RHCP; (d) LHCP. (e, f) Switching of triangle image: (e) input substrate surface covered with cycloidal lens towards the beam, RHCP, beam was focused, (f) substrate was rotated on 180º, RHCP, beam was defocused.

Figure 5 shows images of text observed without any WL lens in the optical path, and with a WL lens and circular polarizer in the optical path. The size of the image at the camera is decreased when the light is RHCP, Figure 5 (b), and increased when the light is LHCP, Figure 5 (c).

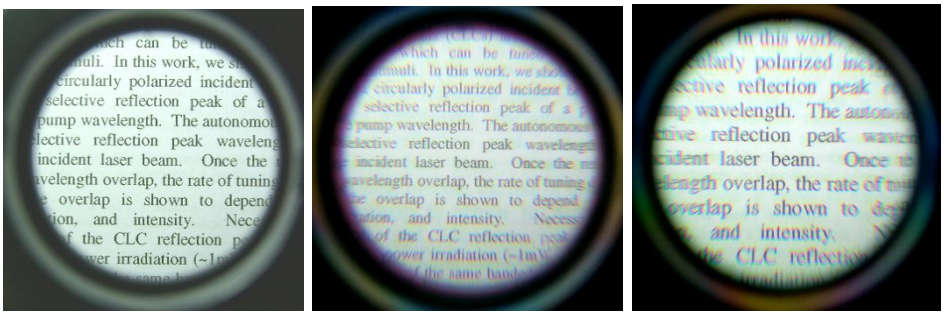

Figure 5. Photos of a book text without WL (a) and with WL (b, c): (b) RHCP, (c) LHCP. Circular polarizer was set between photocamera and the lens.

Waveplate lenses had chromatic aberration like cycloidal diffractive waveplate CDW [17]. For a WL designed for high efficiency in the red region of the spectrum, Figure 6 demonstrates that the half-wave phase retardation condition was satisfied exactly for a red wavelength, but not for wavelengths of used Argon laser, 457, and 514 nm. For blue and green wavelengths, the deviation of the optical retardation from the half-wave condition results in some leakage of undiffracted light through the lens. For the red wavelength, nearly 100% of the light is diffracted, so the red light is nearly all focused

in Figure 6(b), and nearly all defocused in Figure 6(c). There is 0-order laser beam together with focused beam at wavelengths: 457 and 515 nm. Nonetheless, polarization switching between positive and negative focal length was observed for all wavelengths. Dependence of focal length on wavelength is shown in Figure 6(d).

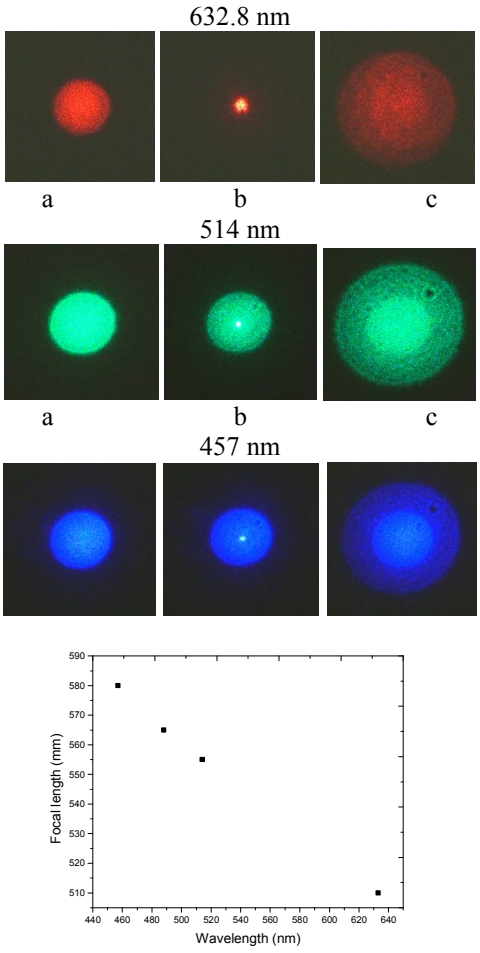

(d)

Figure 6. Photos of images of red laser beam, λ=633 nm, and an Argon laser beams at λ=457 nm and λ=514 nm taken on a screen in focal plane of WL: (a) no WL in set-up, laser beam was expanded and collimated; (b) RHCP, beam was focused; (c) LHCP, beam was defocused. (d) Spectral dependence of focal length.

We used original WL1 to print waveplate lens on another PAAD coated substrate. Original WL and PAAD coated substrate were set in the same holder as close as possible to each other. Printed waveplate lens had focal length a factor of two shorter than that of the original lens.

3.3. Optics of two waveplate lenses

Two waveplate lenses of the same aperture diameter and the same focal length were tested with a collimated input probe red laser beam, with test results shown in Figure 7. The axial location of the screen on which the beam was projected was adjusted with only WL1 in place, with the circular polarization at the input set such that the focal length of WL1 was positive, and with the screen at the focal point of the lens. In Figure 7 (a) the waveplate patterns of the two lenses were facing the same way with axial spacing small compared with the focal length. If the input circular polarization was set such that the focal length of lens WL1 was positive, then the focal length of lens WL2 was negative taking into account that the waveplate lens changes the handedness of circular polarization due to the half wave of optical retardation introduced by lens WL1. For this case, the focal length of WL2 for any given polarization is the inverse of the focal length

of lens WL1, so the combination of the two lenses has essentially no effect on the beam, which remains collimated at the output of the lens pair regardless of the polarization of the input beam.

In Figure 7 (b) the same two waveplate lenses were arranged such that the waveplate patterns on the two lenses were facing in opposite directions. For this arrangement, the focal lengths of the two lenses were the same for a given input beam. The absolute value of the focal length of the combination of the two lenses was one-half the focal length of each of the lenses separately. For the input circular polarization for which the focal lengths were both positive, the focal length of each lens separately was 480 mm, and the focal length of the two lenses together with negligible axial spacing was 240 mm.

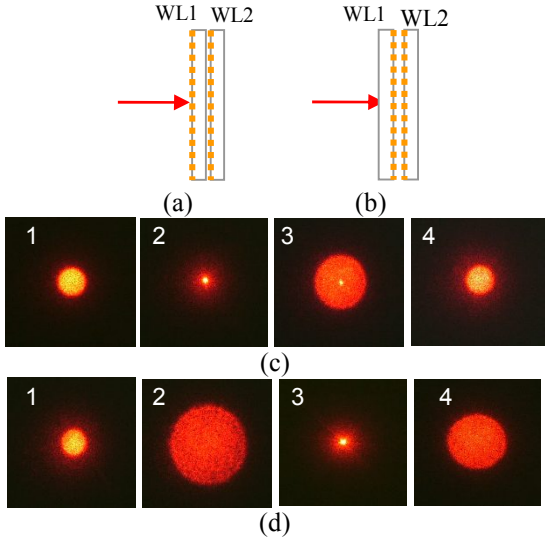

Figure 7. (a, b) Schematic drawing of two WLs. (c, 1-4; d, 1-2) Waveplate lenses were set at distance 480 mm corresponded to focal length of single lens: (c, 1) Laser beam without lenses; (c, 2) single lens WL1 in set-up, input circular polarization adjusted such that the focal length of WL1 is positive, RHCP; (c, 3) single WL1 in set-up, LP; (c, 4) two lenses in set-up, waveplate patterns facing the same way (a), output beam is collimated as for circular polarization as for linear one; (d, 1-2) both lenses WL1 and WL2 in set-up, case (b): (d, 1) RHCP, (d, 2) LHCP. (d, 3-4) Distance between the lens and screen is 240 mm, two lenses in set-up, case (b): (d, 3) RHCP; (d, 4) LHCP.

3.4. Electrical control of focal length

The focusing conditions can be controlled by using electrically controlled phase retardation plates to modulate the polarization state and distribution in the input light. Rotation of quarter waveplate allowed switching between right- and left-handed circular polarized laser beams that resulted in switching the sign of the focal length of any WL lens. We used NLC retarder of thickness L=1.9 μm to create electrically controlled half-wave plate. NLC cell was filled with nematic liquid crystal 6CHBT (from AWAT, Poland). NLC retarder had a retardation of one half wave in its initial state for red wavelength (633 nm). If initially the input circular polarization was set such that the focal length of the WL was negative, the LC retarder switched the sign of the focal length from negative to positive. An AC voltage of 10 V at a frequency of 1 kHz was used to switch the sign of the focal length, Figs. 8(a) – 8(c). If the input circular polarization was adjusted so the WL lens focal length was positive and LC retarder was set, waveplate lens focal length was switched to negative, Figs. 8(d) – 8(f).

Switching between collimated and focused beam was achieved with two waveplate lenses and LC retarder between them. Figure 9 demonstrates beam switching. Initially input lens WL1 had a positive focal length for LHCP light, and lens WL2 had a negative focal length for such light (see Fig. 7, case (b)). Both lenses had a focal length of 240 mm. When LC retarder was set between lenses, WL2 was switched to a negative focal length and the combination of the two lenses collimated the laser beam. When an AC voltage of 10 V was applied, WL2 was switched to a positive focal length and both lenses together focused the laser beam at a distance of 240 mm. Photos in Figs. 9(b) and 9(c) demonstrate this effect.

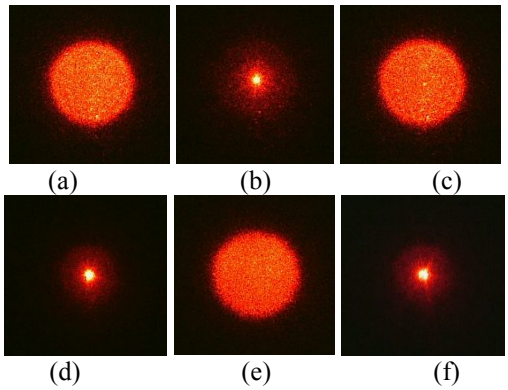

Figure 8. Beam images on a screen in the focal plane. (a) no LC retarder, negative focal length; (b) LC retarder in set-up, no voltage, positive focal length; (c) LC retarder, U=10 V, negative focal length. (d) no LC retarder, positive focal length; (e) LC retarder in set-up, no voltage, negative focal length; (f) LC retarder, U=10 V, positive focal length.

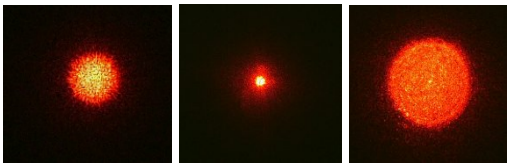

Figure 9. Switching between collimated and focused/defocused beams. (a) Two lenses and LC retarder between them collimated laser beam. U=0V. (b) LHCP. Voltage 10V was applied. Focused beam at distance 240 mm. (c) RHCP. Defocused beam at distance 240 mm. U= 10 V.

Switching effect was observed with WL in thin 2-μm thick LC cell. Polarization pattern was recorded in empty cell on both PAAD coated substrates, after this, the cell was filled with LC 6CHBT. When voltage was not applied to the substrates, laser beam was focused or defocused with LC WL depending on position of input quarter waveplate. When voltage was applied to the substrate, two waveplate lenses collimated the laser beam.

3.5. Free-form waveplate lenses

Free-form patterns in LC cell and LCP were recorded as well. Figure 10 demonstrates recorded structures observed upon inverted Olympus microscope between crossed polarizers.

Figure 11 shows photos of a laser beam focused with a free-form waveplate lens for different polarization states: linear, right-hand circular, and left-hand circular. Diffraction patterns of a red laser beam on above structures are shown at different conditions. The focal length of WL was 860 mm, Figs. 11(a) – 11(c), and 75 mm, Figs. 11(d) – 11(k). Photos in Figs. 11((a) – 11(c) and Figs. 11(d) – 11(f) are obtained in its focal plane. Photos in Figs. 11(g) – 11(k) correspond to far zone. Photos in (a), (d) and (g) correspond to linear polarized incident light. Photos (b), (e), (h) correspond to left-hand circular polarized incident beam. The photos (c), (f), (k) correspond to right-hand circular polarized incident beam**.** 0-order laser beam, which is observed in photos (d) - (k), is due to disturbance of half-waveplate condition for 633-nm wavelength.

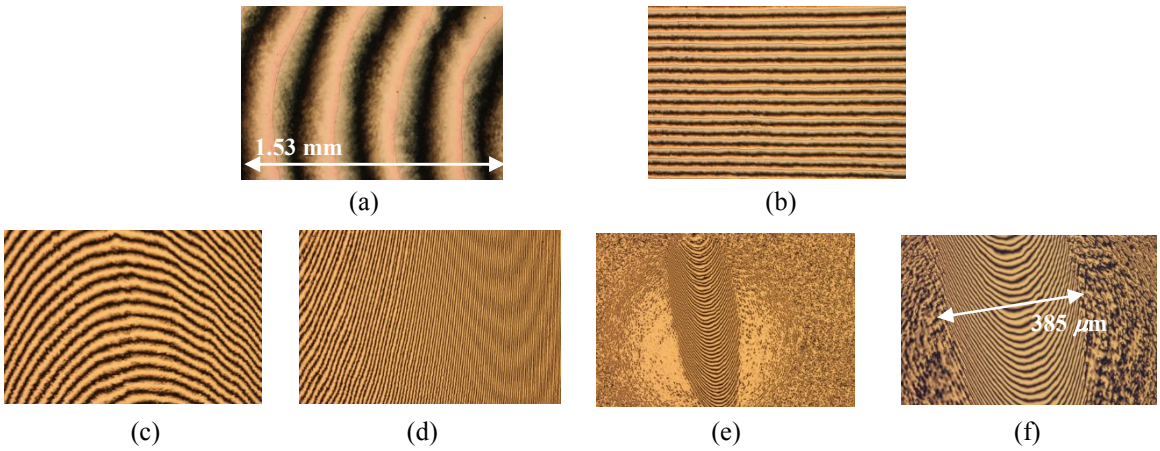

Figure10. (a-b) Photos of recorded pattern in LC layer taken with 10X Olympus objective in different areas. Lens size was 7 mm, spacing period was (a) Λ= 340 μm in the center and (b) Λ= 64 μm on the edge, F=570 mm. (c-f) Lenses in LCP: (c) lens size is 3 mm, spacing period is (c) Λ= 75 μm in the center and (d) Λ= 18 μm on the edge, F=75 mm; (e, f) photos of smaller 0.385 mm waveplate lens taken with (e) 10X and (f) 20X objectives. F=5 mm.

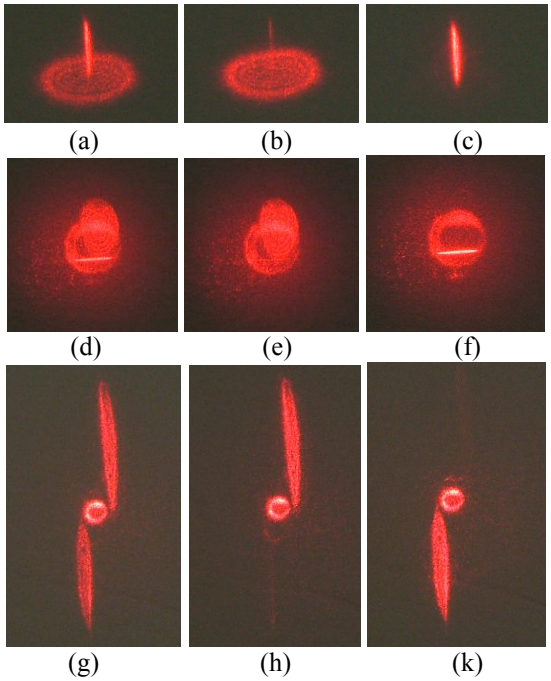

Figure 11. (a-c) Focusing/defocusing of red laser beam with WL of focal length F=860 mm. (d-k) Images of red laser beam focused or defocused with waveplate lens of 75-mm focal length. Photos (d-f) correspond to the focal plane; photos (g) – (h) correspond to far zone. Beam polarization was: (a, d, g) LP; (b, e, h) RHCP; (c, f, k) LHCP.

4. CONCLUSION

The recent development of precise methods for creating photoalignment layers with nearly arbitrary spatial patterns now allows the fabrication of a new generation of optical devices consisting of a micron-thick layers of anisotropic optical material such as liquid crystal polymers with spatially-patterned optical axis orientation. The diffraction efficiency of such components has been demonstrated to be near 100% for a single polarization of light. Such layers can be formed on a variety of substrates. We have demonstrated such techniques by fabricating and testing waveplate lenses and lens arrays, and we have demonstrated electrical switching of the sign of the focal length of such lenses by means of a switchable half-wave plate. We have also demonstrated that a suitably designed pair of waveplate lenses can focus light of any polarization to the same point.

ACKNOWLEDGEMENTS

The work was supported by funding from US Army Natick Soldier Research, Development and Engineering Center. We thank Dr. S. Nersisyan and Dr. H. Xianyu for assistance with LCP coating.

REFERENCES

[1] Born, M. and Wolf, E., *Principles of Optics*, Pergamon Press & Oxford (1975).
[2] Sarkissian, H., Park, B., Tabirian, N. and Zeldovich, B., "Periodically aligned liquid crystal: potential application for projection displays," Mol. Cryst. Liq. Cryst. 451(1), 1–19 (2006).
[3] Katz, M, *Introduction to Geometrical Optics*, World Scientific Publishing Co. Pte. Ltd. (2002).
[4] Nikolova, L. and Ramanujam, S., *Polarization Holography*, Cambridge University Press (2009).
[5] Sato, S., "Liquid-crystal lens-cells with variable focal length," Jpn. J. Appl. Phys. 18(9), 1679-1684 (1979).
[6] Suyama, S., Date, M. and Takada, H., "Three-dimensional display system with dual-frequency liquid-crystal varied focal lens," Jpn. J. Appl. Phys. Part 1**,** 39(2R), 480-484 (2000).
[7] Kelly, T. L., Naumov, A. F., Loktev, M. Yu. and Rakhmatulin, M. A., "Focusing of astigmatic laser diode beam by combination of adaptive liquid crystal lenses," Opt. Commun. 181(4), 295-301 (2000).
[8] Hain, M., Glockner, R., Bhattacharya, S., Dias, D., Stankovic, S. and Tschudi, T., "Fast switching liquid crystal lenses for a dual focus digital versatile disc pickup," Opt. Commun. 188(5), 291-299 (2001).
[9] Lucchetta, D. E., Karapinar, R., Manni, A. and Simoni, F., "Phase-only modulation by nanosized polymer-dispersed liquid crystals," J. Appl. Phys. 91(9), 6060–6065 (2002).
[10] Wang, B., M. Honma, M. Ye, Nose, T. and Sato, S., "Liquid crystal lens with spherical electrode," Jpn. J. Appl. Phys. 41(11A), L1232 –L1233 (2002).
[11] Ren, H., Fan, Y. H. and Wu S. T., "Tunable Fresnel lens using nanoscale polymer-dispersed liquid crystals," Appl. Phys. Lett. 83(8), 1515-1517 (2003).
[12] Ren H. and Wu, S. T., "Adaptive liquid crystal lens with large focal length tunability," Opt. Express 14(23), 11292-11298 (2006).
[13] Sarkissian, H., Serak, S. V., Tabiryan, N. V, Glebov, L B., Rotar, V., Zeldovich, B. Ya., "Polarization-controlled switching between diffraction orders in transverse-periodically aligned nematic liquid crystals," Opt. Lett. 31(15), 2248-2250 (2006).
[14] Serak, S., Tabiryan, N., Zeldovich, B., "High efficiency 1.5 μm-thick optical axis grating and its use for laser beam combining," Opt. Lett. 32(2), 169-171 (2007).
[15] Nersisyan, S. R., Tabiryan, N. V., Hoke, L., Steeves, D. M. and Kimball, B. R., "Polarization insensitive imaging through polarization gratings," Opt. Express 17(3), 1817–1830 (2009).
[16] Hrozhyk, U., Nersisyan, S., Serak, S., Tabiryan, N., Hoke, L., Steeves, D., Kimball, B., "Optical switching of liquid-crystal polarization gratings with nanosecond pulses," Opt. Lett. 34(17), 2554-2556 (2009).
[17] Tabiryan, N. V., Nersisyan, S. R., Steeves, D. M. and Kimball, B. R., "The promise of diffractive waveplates," Opt. Photon. News 21(3), 41–45 (2010).
[18] Tabiryan, N. V., Nersisyan, S. R., White, T. J., Bunning, T. J., Steeves, D. M. and Kimball, B. R., "Transparent thin film polarizing and optical control systems," AIP Advances 1(2), 022153 (2011).
[19] Serak, S., Hakobyan, R., Nersisyan, S., Tabiryan, N., White, T., Bunning, T., Steeves, D. and Kimball, B., "All-optical diffractive/transmissive switch based on coupled cycloidal diffractive waveplates," Opt. Express 20(5), 5460-5469 (2012).
[20] Karimi, E., Slussarenko, S., Piccirillo, B., Marrucci, L., Santamato, E., "Polarization-controlled evolution of light transverse modes and associated Pancharatnam geometric phase in orbital angular momentum," Phys. Rev. A 81(5), 053813 (2010).
[21] Crawford, G. P., Eakin, J. N., Radcliffe, M. D., Callan-Jones, A. and Pelcovits, R. A., "Liquid-crystal diffraction gratings using polarization holography alignment techniques," J. Appl. Phys. 98(12), 123102 (2005).